Optical Control of Aggregation Induced Emission Shift by Photoisomerizable Precipitant in a Liquid Droplet Microresonator

*Shuai Zhao, Hiroshi Yamagishi, Yasuo Norikane, Shotaro Hayashi, Yohei Yamamoto**

S. Zhao, Dr. H. Yamagishi, Prof. Y. Yamamoto
Department of Materials Science, Faculty of Pure and Applied Sciences, and Tsukuba Research Center for Energy Materials Science (TREMS), University of Tsukuba, 1-1-1 Tennodai, Tsukuba, Ibaraki 305-8573, Japan
E-mail: yamamoto@ims.tsukuba.ac.jp

Dr. Y. Norikane
Research Institute for Advanced Electronics and Photonics, National Institute of Advanced Industrial Science and Technology (AIST), Central 5, 1-1-1 Higashi, Tsukuba, Ibaraki 305-8565, Japan

Prof. S. Hayashi
School of Environment Science and Research Center for Molecular Design, Kochi University of Technology, 185 Miyanokuchi, Tosayamada, Kami, Kochi, 782-8502, Japan

Keywords: droplet resonator, photoisomerization, fluorescence switch, azobenzene, aggregation-induced emission shift

Abstract

Emission-switchable fluorophores often include stimuli-responsive units in their molecular structures. This strategy works well, but the applicable compounds have been limited to the derivatives of several kinds of photochromic molecules such as diarylethene, azobenzene, and spiropyran. Here we present a simple methodology based on a photoresponsive precipitant for achieving color-switchable photoluminescence. A luminescent dye, cyano-substituted oligo(phenylenevinylene) (COPV), features both twisted intramolecular charge-transfer and aggregation-induced emission shift properties, leading to the change in the luminescence color from green to red upon precipitation. The COPV, together with photoisomerizable precipitant azobenzene (C6), is doped into spherical droplets of epoxy resin (ER) in a liquid state. The photoisomerization of C6 induced by UV-irradiation and heating alternatively precipitates out and dissolves COPV in ER and changes the photoluminescence color, while maintaining the

optical microresonator properties. This study will open a promising way for assembling/disassembling novel emission color-switchable systems.

1. Introduction

Developing organic luminescent materials attracts growing research interest due to their tunable and reversible emission and potential applications in optical communication, organic light-emitting diodes, and chemical/biological sensors. Unlike conventional fluorophores that show aggregation-caused quenching (ACQ), aggregation-induced emission (AIE) process has been discovered by Tang's group, [1] in which a series of molecules are weakly emissive in the molecularly dissolved state but become highly emissive in the aggregated or the solid state because of the restriction of the intramolecular motion. In the past decades, tremendous progress has been achieved in tuning the emission of AIE-luminogens (AIEgens) through ligand modification.[2–4] As the family of AIE-active molecules developed, a new series of aggregation-induced emission shift (AIES) molecules combining twisted intramolecular charge transfer (TICT) and AIE has been reported for dual-state emission fluorophores.[5–7]

Even though the emission color can be manipulated by controlling the molecular configuration and forming their single crystal with different aggregation states, dynamically tuning the emission color is still challenging and highly desirable. Recently, a series of AIEgens is widely utilized as mechanofluorochromic (MFC) materials which are dependent on changes in their physical molecular packing modes.[8] Typically, photoluminescence (PL) color of AIES-luminogens (AIESgens) varies by adding nonsolvent into the well-dissolved solution to induce its aggregation. We envision that switching the emission color could be easily achieved with liquid microresonators doped with AIEgens and triggering the aggregation process by a photoresponsive precipitant (Scheme 1).

Azobenzene, a conventional photoisomerizable molecule, has a wide range of applications in many fields such as information storage,[9] energy storage,[10,11] and surface modification.[12,13] Azobenzene exists in two stereo-configurations, stable *trans*- and metastable *cis*- configurations. It has been known that the change in the molecular configuration of azobenzene leads to significant differences in the physicochemical properties of the host materials in terms of surface wettability[14,15] or thermodynamic stability.[16,17] Recently, a new kind of photoisomer showing phase transition from solid to liquid is reported.[18–20] The solid-liquid reversible conversion as a light-controlled molecular switch enables selective etching of surfaces.[21] Azobenzene can also be used to functionalize oligomers, in which azobenzene crystallization play an important role in the self-assembly of 2D monolayer structure.[22] Along this line, switching emission color is expected to be achieved by photoisomerization-induced aggregation of AIESgens in liquid.

Whispering gallery mode (WGM) microresonators, which feature high quality (Q) factor and small mode volume, have been exploited for their potential applications, such as multi-color laser,[23–26] biological or chemical sensing,[27–30] information encryption[31–33] and integrated optics.[34,35] As a promising platform to enhance the light-matter interaction, the detailed information about the optical cavity and gain medium inside can be easily characterized by recording the resonant spectrum.[36] A few liquid-based tunable microresonators have been reported, whose resonant peak shift is induced by mechanical deformation or changing the refractive index (RI).[37]

In this paper, we develop color-switchable system with AIESgens (cyano-substituted oligo(phenylenevinylene), COPV, Figure 1a) doped spherical droplets. The PL color of COPV varies from green to yellow and red upon controlling the twisted intramolecular charge transfer (TICT) and AIE processes. By incorporating photoisomerable azobenzene (C6, Figure 1b) into COPV doped epoxy resin (ER), switchable PL is achieved. C6 shows the phase transition between solid *trans*-isomer and liquid *cis*-isomer during photoisomerization, corresponding to

UV and visible light irradiation. Due to the difference in the solubility of COPV in ER and *cis*-C6, photoisomerizable C6 acts as precipitant triggering the aggregation of COPV and switching PL wavelength (as shown in Scheme 1). Heating promotes the redissolution of COPV in ER and reverts the color to the initial state. After spraying ER onto a hydrophobic substrate, the resultant spherical droplet ($MS_{ER\text{-}C6}$) shows WGM resonance in the PL spectrum. The resonant PL color can be switched between green and yellow by irradiation with UV or heating.

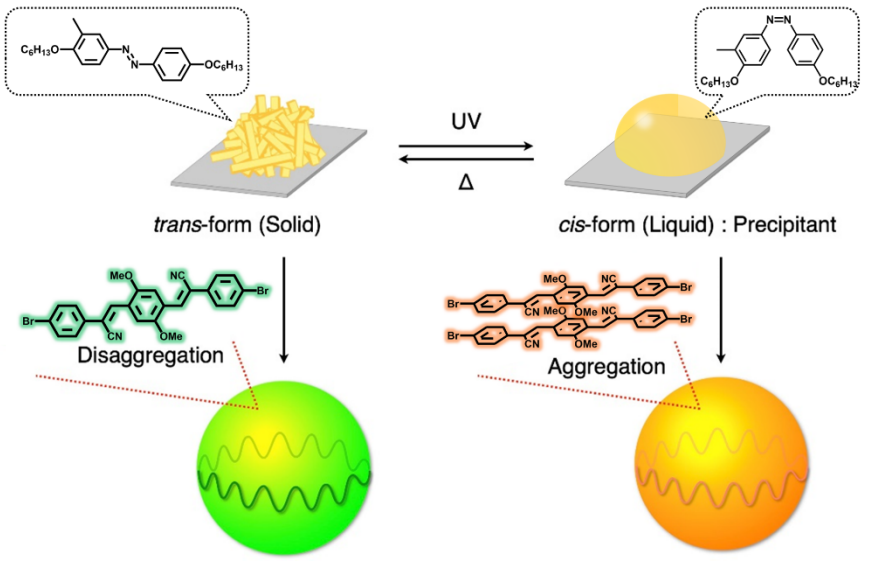

Scheme 1. Optical control of aggregation/disaggregation of AIES-luminogen in an epoxy resin (ER) droplet microresonator by photoisomerization of azobenzene derivative that acts as precipitant in its *cis*-form.

2. Results and Discussion

2.1. Aggregation-induced emission properties of COPV

First, we study the fluorescence properties of COPV (1 mM) in solvents with varying polarity. When dissolved in toluene, COPV emits green fluorescence with a unimodal emission band (Figure 1c, red line) centered at 507 nm, displaying a 75 nm stokes shift (Figure S1). As the solvent polarity increases (*e.g.* dichloromethane, tetrahydrofuran, dimethylformamide, and dimethyl sulfoxide), the emission of COPV red shifts weakly accompanied by decreased emission intensity, which is in line with the features of the TICT effect. To prove the AIE property, the fluorescence characteristics of COPV (1mM) are investigated in THF/water

mixtures (water fraction (f_w) from 0 to 90%, v/v). As shown in Figure 1d–f, COPV emits green fluorescence in pure THF, indicating a well-dispersed monomer state, assigned as G-phase (Figure 1e). When adding water into the THF solution (f_w from 0 to 40%), the emission of COPV red shifts along with weakened intensity, which is the characteristic of TICT induced by the increased polarity of the THF/water mixture.[38–40] Upon increasing f_w to 50%, the fluorescence intensity at the green region is suppressed progressively. At the same time, aggregates of COPV (assigned as Y-phase, Figure 1e) form in the mixture due to its insolubility in water, and a new emission band appears in the yellow-color region with a maximum wavelength (λ_{em}) of 559 nm. The origin of this new emission band is assumed to be the restricted intramolecular vibrational and rotational motions in the aggregated COPV, which leads to the slow nonradiative relaxation and higher fluorescence quantum yield in the solid state.[41] The molecular configuration of the Y-phase is presumed to be twisted edge-to-face stacking, according to previous publication.[42] After further addition of water, the emission bathochromic shift to 603 nm due to the high extent of aggregation (assigned as R-phase, Figure 1e), in which planar COPV stacks on one another via π–π interactions.[42,43] The relatively stronger emission intensity results from the increased extent of aggregation and the stronger restriction of the intramolecular vibrational and rotational motions.[39] Unlike conventional AIEgens that hardly emit fluorescence in the monomer state and are highly emissive in the aggregated state,[44] COPV exhibits a change in color from green to yellow and red region; the corresponding maximum emission wavelengths are 510 nm, 559 nm, and 603 nm, respectively, which is highly advantageous for fabricating color tunable microresonators.

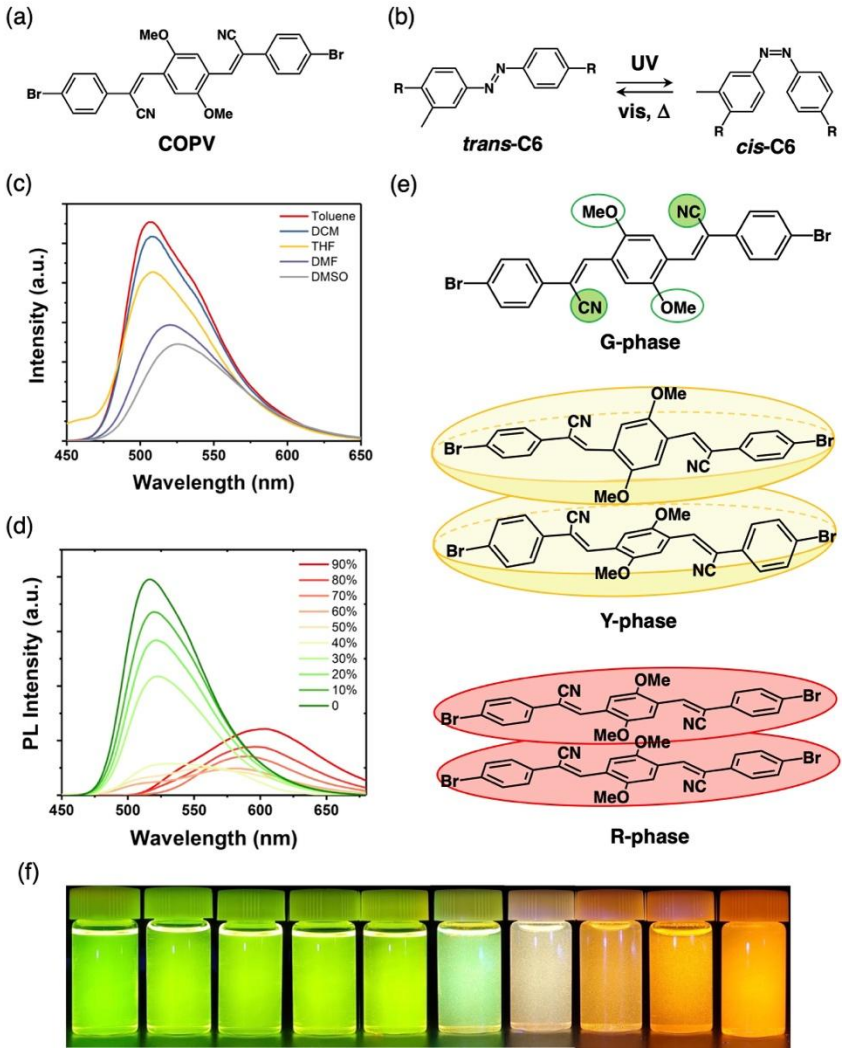

Figure 1. a) Molecular structure of COPV. b) Molecular structure of C6 in *trans* (left) and *cis* (right) forms. c) PL spectra of COPV (1mM) in various solvents. d) PL spectra of COPV (1mM) in THF/water mixture with various mixing ratios. e) Proposed molecule configuration of COPV in G-, Y-, and R-phases. f) Photographs of COPV in THF/water mixtures under UV-LED illumination (λ_{ex} = 375 nm).

2.2. Color-switchable liquid ER film

To tune the emission color of COPV, liquid epoxy resin (ER) is utilized as a matrix to fabricate COPV doped liquid film. The droplet of ER doped with COPV shows green emission (Figure S2), meaning the good dispersion of COPV in ER. On the contrary, COPV aggregates and shows red emission when doped in PDMS (Figure S3). Furthermore, photoisomer azobenzene (C6, the chemical structure shown in Figure 1b) is also added to the COPV/ER

mixture to realize a photochemically switchable system for inducing the AIE of COPV. *Trans*-form C6 (*trans*-C6) is in the solid state but changes to the liquid state when photoisomerizes to *cis* form (*cis*-C6).[20] The photoisomerization and corresponding solid/liquid phase transition can be achieved by shining UV/blue light that excites the absorption band of *trans*-C6 (Figure S1). We first explore the photoisomerization of C6 in the liquid ER droplet to analyze their compatibility. (Figure S4). Herein, the powder of *trans*-C6 is directly mixed into ER. Photoisomerization of *trans*-C6 occurs quickly within 1 min of UV light irradiation. In addition, liquid *cis*-C6 is totally miscible with ER. Upon visible light irradiation, *cis*-C6 isomerizes to *trans*-C6, and the solid *trans*-C6 separates from ER, floats, and covers the surface of the ER droplet.

The role of C6 in the mixture system is studied by directly adding *cis*-C6 to COPV/ER mixture. Figure S5b shows fluorescent microscope (FM) images of a drop-cast liquid film of ER/*cis*-C6/COPV. Obviously, COPV in the liquid film tends to crystallize with the increased ratio of *cis*-C6 to epoxy resin like the phenomenon in THF/water solution of COPV, indicating low solubility of COPV in liquid *cis*-C6. Therefore, adding *cis*-C6 or photoisomerization from solid *trans*-C6 to liquid *cis*-C6 induces the aggregation of COPV in the ER medium.

The photoinduced color switching property of a drop cast liquid film of ER/*trans*-C6/COPV is investigated using FM microscopy. As shown in Figure S6, the drop cast liquid film displays green-color emission under irradiation at 450–490 nm. Then the film was irradiated with UV light (λ_{ex} = 350–390 nm) for 30s, during which *trans*-C6 is converted into *cis*-C6. The liquid form of *cis*-C6 decreases the solubility of COPV in ER, leading to the aggregation of COPV to form micro-crystals with red-color emission under irradiation at 450–490 nm. Furthermore, XRD patterns of the liquid film of ER/*trans*-C6/COPV before and after irradiation with UV light are also recorded (Figure S7), in which a set of diffraction peaks appears after UV irradiation that corresponds to those from COPV powder. The color-switching property of drop-cast liquid film is further confirmed by using an octagonal aperture as a

photomask (Figure 2a). Only *trans*-C6 at this octagonal area is photoiomerized to *cis*-C6 after the UV light irradiation, and COPV at this octagonal area aggregates to form micro-crystals. Figure 2b–e shows that, after UV light irradiation for 60 s, COPV at the octagonal area crystallizes and shows red color fluorescence. It should be noted that *cis*-C6 is converted into *trans*-C6 during the observation of FM images under irradiation at 450–490 nm, indicating that photoisomerization of C6 with the phase transition from liquid to solid state hardly induces the disaggregation of COPV.

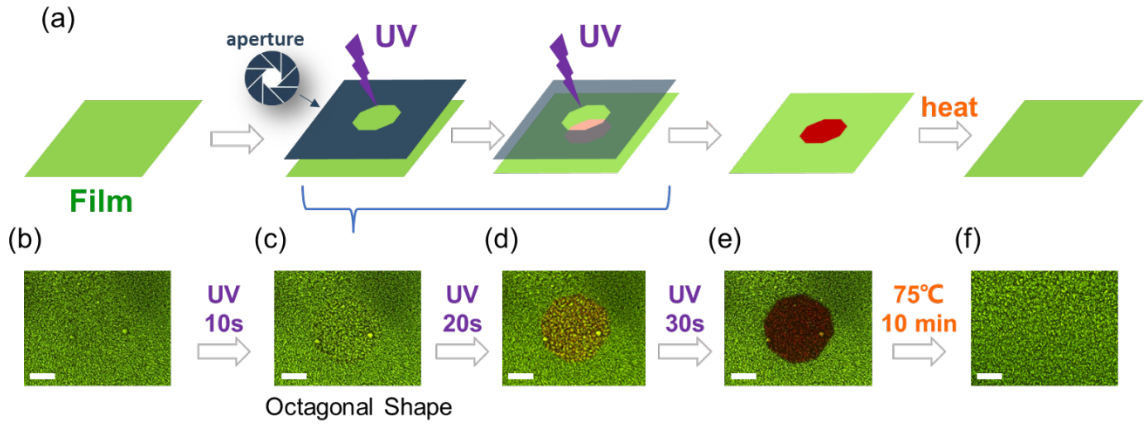

Figure 2. a) a) Schematic representation of the color-change experiments by UV irradiation through an octagonal aperture to ER droplet film doped with *trans*-C6 and COPV. b–f) FM images of the droplet film upon UV irradiation and subsequent thermal annealing (scale bar: 150 μm).

The dissolution of aggregated COPV microcrystals in ER is feasible but slow due to ER's high viscosity. Thermal annealing decreases the viscosity of ER (Figure S8) which promote dissolution of COPV in ER. This phenomenon is confirmed by a thermal annealing experiment, during which COPV powder is put in an epoxy resin droplet and dissolved in epoxy resin by heating the droplet (Figure S9). In Figure 2f, the aggregated COPV microcrystals at the octagonal area are dissolved again in the liquid ER film by annealing the film at 75 °C for 10 min. As a result, the fluorescent color turns back to green. It should be mentioned that the *cis*-to-*trans* isomerization process also occurs during annealing, which also assists in the

increase of the solubility of COPV in ER. Accordingly, the green emission color maintains even after cooling at room temperature.

2.3. Color-switchable microresonators

To obtain color-switchable microresonators, a spherical microdroplet (**MD$_{ER-C6}$**) is prepared by spraying a THF solution of a mixture of ER, C6, and COPV onto a superhydrophobic substrate (see the experiment section) with diameters (*d*) of 5–30 μm **(**Figure S10). The resultant **MD$_{ER-C6}$** shows green-color PL upon photoirradiation at λ_{ex} = 450–490 nm (Figure 3a). From Figure 3b, the contact angle of epoxy resin droplet on hydrophobic film can be calculated to be ~103°, which makes it possible to entrap light at its outermost surface via total internal reflection. Upon excitation with a focused laser beam (λ_{ex} = 455 nm, see the Experimental section) at the rim, a single **MD$_{ER-C6}$** with *d* = 11.4 μm displays periodic PL peaks that are superposed on a broad green PL band (Figure 3c), which can be attributed to WGM resonance induced by the light confinement at the polymer/air interface. As *d* increases, the spacing between adjacent WGM peaks (free spectral range, FSR) decreases because of the longer optical path, which is in line with the equation for WGM resonator,

$$\lambda^2/FSR = n\pi d \qquad (1)$$

where *n* is the refractive index of the medium. A plot of λ^2/FSR as a function of *d* (Figure 3d) from a series of single **MD$_{ER-C6}$** with *d* of 6–20 μm shows a linear relationship, which is as similar as the results for polystyrene microspheres doped with COPV as fluorescent dopant (Figures S11 and S12).

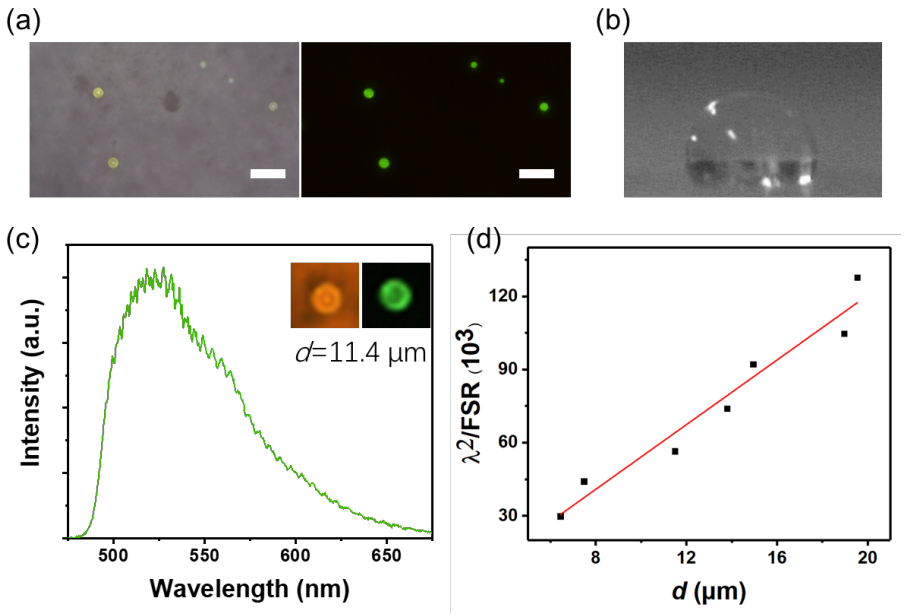

Figure 3. a) Optical and FM images of $\mathbf{MD_{ER\text{-}C6}}$. (Scale bar: 100 μm) b) contact angle of ER on a hydrophobic substrate. c) PL spectra of a single $\mathbf{MD_{ER\text{-}C6}}$. Insets show optical and FM images of $\mathbf{MD_{ER\text{-}C6}}$. d) Plot of λ^2/FSR versus *d*. The red line represents the least squares fitting with a linear correlation.

WGM PL of $\mathbf{MD_{ER\text{-}C6}}$ upon aggregation/disaggregation of COPV inside the droplet is further investigated. The spectra of a single $\mathbf{MD_{ER\text{-}C6}}$ displaying WGM resonance are recorded before and after irradiation with UV-LED light (λ = 375 nm) for 1 min (Figure 4). The UV irradiation gives rise to the aggregation of COPV, accompanying the shift of the broad PL band from green to yellow region. By comparing the spectrum, it can be observed both the FSR before and after irradiation are 4.02 nm (Figure S13), indicating that the size and refractive index of the $\mathbf{MD_{ER\text{-}C6}}$ cavity hardly change upon aggregation of COPV in the ER droplet. The reversion of the PL color from yellow to green is also demonstrated by heating $\mathbf{MD_{ER\text{-}C6}}$ at 75°C for 10 min and then cooling to 25 °C. From the PL spectrum, the broad PL band shifts back to the green region along with WGM resonant peaks due to the redissolved COPV in $\mathbf{MD_{ER\text{-}C6}}$.

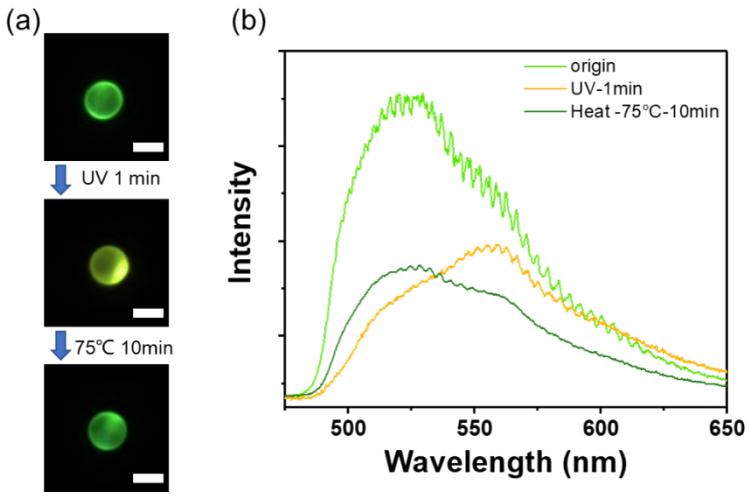

Figure 4. a) FM images and b) μ-PL spectra of $\mathbf{MD_{ER\text{-}C6}}$ before and after UV irradiation for 1 min. and subsequent thermal annealing at 75 °C (scale bar: 10 μm).

To confirm the redissolution of COPV in $\mathbf{MD_{ER\text{-}C6}}$ and the corresponding emission color shift from yellow to green, a direct heating experiment of COPV microcrystal inside the spherical microdroplet of ER ($\mathbf{MD_{ER}}$) is demonstrated. By using a micro-manipulator equipped with a sharp tungsten needle, a small grain of the microcrystal of COPV is directly put into $\mathbf{MD_{ER}}$ (Figure S14). After heating at 75 °C for 10 min, the COPV microcrystal is dissolved in $\mathbf{MD_{ER}}$. The $\mathbf{MD_{ER}}$ displays green emission upon photoirradiation at λ_{ex} = 450–490 nm, while the surrounding microdroplets still show no emission. The μ-PL spectrum of this $\mathbf{MD_{ER}}$ exhibits a set of periodic peaks mainly overlapping on the green region band, which is attributed to G-phase COPV in $\mathbf{MD_{ER}}$.

3. Conclusion

In conclusion, we develop a new approach for switching the fluorescence color by solubility change of fluorescent dye (COPV) upon photoisomerization of the second dopant C6. The photoisomerization induces solid-to-liquid phase transition, leading to the decrease of the solubility of COPV in epoxy resin and inducing the emission shift by aggregation. This strategy

works well even in a micrometer-scale liquid droplet optical resonator of epoxy resin, in which aggregation/disaggregation of COPV occurs upon photoisomerization of C6 by UV irradiation/heating, resulting in a large fluorescence spectral shift that involves whispering gallery mode fingerprint, while maintaining the size and refractive index of the droplet resonator. This study will open a new way for the design of emission-color tunable systems and other optical devices.

4. Experimental Section

Chemicals. COPV and C6 were synthesized according to reported procedures.[20,45] Epoxy Resin was purchased from PT. Bratachem, Bandung. HIREC®1450NF was purchased from NTT Advanced Technology Corporation. All other reagents and solvents were used as received. COPV microcrystals were synthesized according to our previous paper.[43]

Preparation of the liquid layer from ER/C6/COPV. ER, C6, and COPV with a weight ratio of 3:2:4 was dissolved in $CHCl_3$. Then, the solution was drop-casted on a quartz substrate. After naturally evaporating $CHCl_3$, the liquid layer of ER/C6/COPV was obtained. To maintain the fluidity of Epoxy Resin, no curing agent was used in this work.

Preparation of spherical droplet $MD_{ER\text{-}C6}$. Superhydrophobic substrate was prepared by spin-coating fluorinated silica nanoparticles (HIREC®1450NF) on a quartz substrate. ER, C6 and COPV were mixed with a weight ratio of 15:10:2, respectively, and dissolved in THF. Then the mixture was sprayed on the hydrophobic substrate with a manual sprinkling can. After naturally evaporating $CHCl_3$, the spherical droplet **$MD_{ER\text{-}C6}$** was obtained.

Preparation of the microsphere $MS_{PS\text{-}COPV}$. COPV-doped polystyrene (PS) microspheres (**$MS_{PS\text{-}COPV}$**) were prepared by miniemulsion method. Typically, an aqueous solution of sodium dodecyl sulfonate (SDS, 30 mg mL^{-1}, 1 mL) was added to a $CHCl_3$ solution (0.1 mL) of COPV with 0.1 mg mL^{-1} and PS with various concentrations. The two-phase-separated solution was emulsified by vigorous stirring with a homogenizer (10k rpm, 5 min). The emulsion was

allowed to stand for 2 days in an atmosphere to evaporate $CHCl_3$ totally. After removing the excess SDS, complete precipitation of **$MS_{PS\text{-}COPV}$** was obtained.

Characterization. For characterizations, one drop (20–30 μL) of the diluted suspension of **$MS_{PS\text{-}COPV}$** was spin-coated on a quartz substrate using a spin-coater for micro-photoluminescence (μ-PL) measurement and on a bare SiO_2/Si substrate for scanning electron microscope (SEM) measurements. SEM microscopy was performed on a Hitachi model S-3700N SEM operating at 30 kV. Optical and fluorescence microscopy observations were carried out using an Olympus model BX53 Upright Microscope. To manipulate the COPV microcrystals, a micromanipulation apparatus (MC104 and micro support model Qp-3RH with input AC100-240V 50/60Hz 140 VA) with an electrically controlled stepping stage and a thin microneedle was used.

μ-PL Measurements. μ-PL measurements were carried out with a homemade μ-PL measurement system. A cw laser (405 or 455nm, CNI model LPS-1) was passed through an ×20 objective lens (NA = 0.5) set on an optical microscope (Nikon model Eclipse LV100) and focused onto a specimen. PL emitted from the specimen was collected with the identical objective lens and detected with a spectrometer (Lambda Vision model LV-MC3/T, grating: 300 grooves mm^{-1}) through an optical fiber with a spectral resolution of 0.12 nm with a 100 μm slit. An additional UV-LED light (λ_{ex} = 375 nm, 3.0 W) was used to irradiate *trans*-C6.

Supporting Information

Supporting Information is available from the Wiley Online Library or from the author.

Acknowledgments

This work was supported by JST CREST (JPMJCR20T4), ACT-X (JPMJAX201J), and FOREST (JPMJFR211W) from Japan Science and Technology Agency (JST), Grant-in-Aid for Scientific Research on Innovative Areas "π-System Figuration" (JP17H05142, JP17H05171) and "Soft Crystal" (JP20H04684), and Scientific Research (A) (JP16H02081) from Japan Society for the Promotion of Science (JSPS).

Received: ((will be filled in by the editorial staff))
Revised: ((will be filled in by the editorial staff))
Published online: ((will be filled in by the editorial staff))

References

[1] J. Luo, Z. Xie, J. W. Y. Lam, L. Cheng, H. Chen, C. Qiu, H. S. Kwok, X. Zhan, Y Liu, D. Zhu, B. Z. Tang, *Chem. Commun.* **2001**, *18*, 1740.

[2] Y. Wang, H. Li, D. Wang, B.Z. Tang, *Adv. Fun. Mater* **2021,** *31*, 2006952.

[3] J. Li, J. Wang, H. Li, N. Song, D. Wang, B.Z. Tang, *Chem. Soc. Rev.* **2020**, *49*, 1144.

[4] X. Han, F. Ge, J. Xu, X.H. Bu, *Aggregate* **2021**, *2*, 28.

[5] R. Hu, C. A. Gómez-Durán, J. W. Lam, J. L. Belmonte-Vázquez, C. Deng, S. Chen, R. Ye, B. Z. Tang, *Chem. Commun*. **2012**, *48*, 10099.

[6] S.A.A. Abedi, W. Chi, D. Tan, T. Shen, C. Wang, E.C.X. Ang, C.H. Tan, F. Anariba, X. Liu, *J. Phys. Chem. A* **2021**, *125*, 8397.

[7] Y.C. Chiang, Z.L. Lai, C.M. Chen, C.C. Chang, B. Liu, *J. Mater. Chem. B* **2018**, *6*, 2869.

[8] Y. Wang, D. Cheng, H. Zhou, J. Liu, X. Liu, J. Cao, A. Han,C. Zhang, *Dyes and Pigments* **2019**, 171, 107739.

[9] C. Zhai, G. Fang, W. Liu, T. Wu, L. Miao, L. Zhang, J. Ma, Y. Zhang, C. Zong, S. Zhang, C. Lu, *ACS Appl. Mater. Interfaces* **2021**, *13*, 42024.

[10] G. D. Han, S. S. Park, Y. Liu, D. Zhitomirsky, E. Cho, M. Dincă, J. C. Grossman, *J. Mater. Chem. A* **2016**, *4*, 16157.

[11] Z. Wang, R. Losantos, D. Sampedro, M. A. Morikawa, K. Börjesson, N. Kimizuka, K. Moth-Poulsen, *J. Mater. Chem. A* **2019**, *7*, 15042.

[12] P. Theamdee, R. Traiphol, B. Rutnakornpituk, U. Wichai, M. Rutnakornpituk, *J. Nanopart. Res*. **2011**, *13*, 4463.

[13] C. Cannizzo, S. Amigoni-Gerbier, M. Frigoli, C. Larpent, *J. Polym. Sci., Part A:*

Polym. Chem. **2008**, *46*, 3375.

[14] Q. Zhou, I. Fursule, B. J. Berron, M. J. Beck, *J. Phys. Chem. A* **2016**, *120*, 7101.

[15] T. Chen, S. Xu, F. Zhang, D. G. Evans, X. Duan, *Chem. Eng. Sci*. **2009**, *64*, 4350.

[16] X. Pang, J. A. Lv, C. Zhu, L. Qin, Y. Yu, *Adv. Mater.* **2019**, *31*, 1904224.

[17] Y. Liu, H. Wang, P. Liu, H. Zhu, B. Shi, X. Hong, F. Huang, *Angew. Chem. Int. Ed*. **2021**, *60*, 5766.

[18] E. Uchida, R. Azumi, Y. Norikane, *Nat. Commun.* **2015**, *6*, 7310.

[19] W. C. Xu, S. Sun, , S. Wu, *Angew. Chem. Int. Ed*. **2019**, *58*, 9712.

[20] G. Fan, S. Wang, J. Jiang, Z. Liu, Z. Liu, G. Li, *Chem. Eng. J.* **2022**, *447*, 137534.

[21] Y. Norikane, E. Uchida, S. Tanaka, K. Fujiwara, E. Koyama, R. Azumi, H. Akiyama, H. Kihara, M. Yoshida, *Org. Lett.* **2014**, *16*, 5012.

[22] R. H. Zha, G. Vantomme, J. A. Berrocal, R. Gosens, B. de Waal, S. Meskers, E. W. Meijer, *Adv. Funct. Mater*. **2018**, *28*, 1703952.

[23] H. Dong, C. Zhang, X. Lin, Z. Zhou, J. Yao, Y. S. Zhao, *Nano Lett.* **2017**, *17*, 91.

[24] M. P. Zhuo, Y. Su, Y. K. Qu, S. Chen, G. P. He, Y. Yuan, H. Liu, Y. C. Tao, X. D. Wang, L. S. Liao, *Adv. Mate.* **2021**, *33*, 2102719.

[25] Y. Du, C. L. Zou, C. Zhang, K. Wang, C. Qiao, J. Yao, Y. S. Zhao, *Light: Sci. Appl.* **2020**, *9*, 1.

[26] J. Liang, M. Chu, Z. Zhou, Y. Yan, Y. S. Zhao, *Nano Lett.* **2020**, *20*, 7116.

[27] S. Zhang, N. Liang, X. Shi, W.hao, T. Zhai, *ACS Appl. Mater. Interfaces* **2021**, *13*, 45916.

[28] X. Cai, Z. Xu, X. Zheng, C. Ran, P. Liu, X. He, X. Jin, Q. Liao, H. Fu, *Chem. Commun.* **2019**, *55*, 814.

[29] G. Q. Wei, Y. Yu, M. P. Zhuo, X. D. Wang, L. S. Liao, *J. Mater. Chem. C* **2020**, *8*, 11916.

[30] Y. C. Chen, Q. Chen, X. Fan, *Optica*, **2016**, *3*, 809.

[31] D. Okada, Z. H. Lin, J. S. Huang, O. Oki, M. Morimoto, X. Liu, T. Minari, S. Ishii, T. Nagao, M. Irie, Y. Yamamoto, *Mater. Horiz.* **2020**, *7*, 1801.

[32] T. Zhang, Z. Zhou, X. Liu, K. Wang, Y. Fan, C. Zhang, J. Yao, Y. Yan, Y. S. Zhao, *J. Am. Chem. Soc.* **2021**, *143*, 20249.

[33] M. P. Zhuo, Y. C. Tao, X. D. Wang, Y. Wu, S. Chen, L. S. Liao, L. Jiang, *Angew. Chem. Int. Ed*. **2018**, 57, 11300.

[34] Hendra, A. Takeuchi, H. Yamagishi, O. Oki, M. Morimoto, M. Irie, Y. Yamamoto, *Adv. Funct. Mater.* **2021**, *31*, 2103685.

[35] Q. Lv, X. D. Wang, L. S. Liao, *Adv. Funct. Mater*. **2022**, 2202364.

[36] G. Q. Wei, X. D. Wang, L. S. Liao, *Laser Photonics Rev.* **2020**, *14*, 2000257.

[37] V. D. Ta, R. Chen, H. D. Sun, *Sci. Rep.* **2013**, *3*, 1.

[38] D. Cheng, D. Xu, Y. Wang, H. Zhou, Y. Zhang, X. Liu, A. Han, C. Zhang, *Dyes and Pigments* **2020**, *173*, 107934.

[39] Y. Ma, Y. Li, L. Chen, Y. Xiong, G. Yin, *Dyes and Pigments* **2016**, 126, 194.

[40] R. Hu, E. Lager, A. Aguilar-Aguilar, J. Liu, J. W. Lam, H. H. Sung, I. D. Williams, Y. Zhong, K. S. Wong, E. Peña-Cabrera, B. Z. Tang, *J. Phys. Chem. C*, **2009**, 113, 15845.

[41] Y. Li, F. Li, H. Zhang, Z. Xie, W. Xie, H. Xu, B. Li, F. Shen, L. Ye, M. Hanif, D. Ma, Y. Ma, *Chem. Commun.* **2007**, *3*, 231.

[42] Y. Xu, K. Wang, Y. Zhang, Z. Xie, B. Zou, Y. Ma, *J. Mater. Chem. C* **2016**, *4*, 1257.

[43] S. Zhao, H. Yamagishi, O. Oki, Y. Ihara, N. Ichiji, A. Kubo, S. Hayashi, Y. Yamamoto, *Adv. Opt. Mater.* **2022**, *10*, 2101808.

[44] Q. Feng, Y. Li, L. Wang, C. Li, J. Wang, Y. Liu, K. Li, H. Hou, *Chem. Commun.* **2016**, *52*, 3123.

[45] S. Hayashi, *Bull. Chem. Soc. Jpn*, **2022**, *95*, 721.

Color-switchable optical resonator is realized from an epoxy resin liquid microdroplet, doped with fluorescent dye cyano-substituted oligo(phenylenevinylene) (COPV) and photoisomerizable azobenzene derivative. The liquid-state *cis*-isomer of the azobenzene works as a precipitant for COPV that leads to aggregation/disaggregation of COPV by optical control, accompanying a large aggregation-induced emission shift in the droplet resonator.

*Shuai Zhao, Hiroshi Yamagishi, Yasuo Norikane, Shotaro Hayashi, Yohei Yamamoto**

Optical Control of Aggregation Induced Emission Shift by Photoisomerizable Precipitant in a Liquid Droplet Microresonator

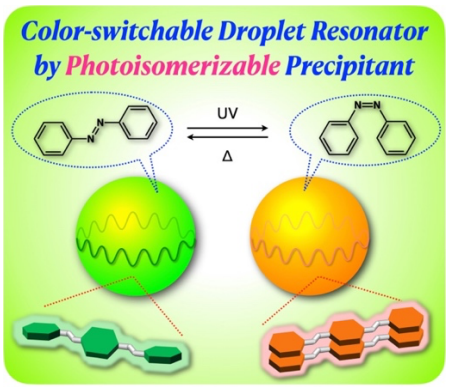

Supporting Information

Optical Control of Aggregation Induced Emission Shift by Photoisomerizable Precipitant in a Liquid Droplet Microresonator

*Shuai Zhao, Hiroshi Yamagishi, Yasuo Norikane, Shotaro Hayashi, Yohei Yamamoto**

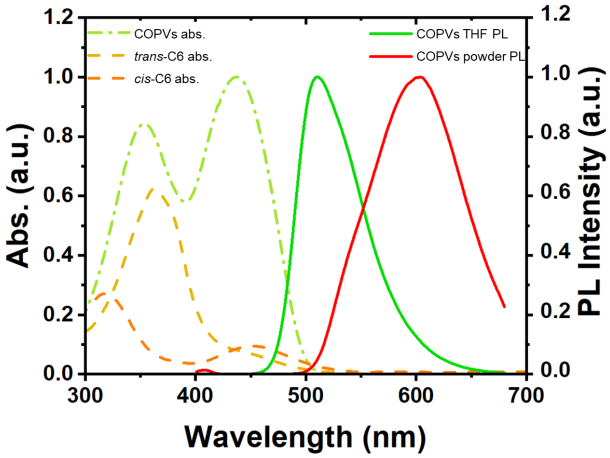

Figure S1. Electronic absorption spectra of COPV and C6 (broken curves) and PL spectra of COPV (solid curves). For concentration, [COPV] = 1 mM, [C6] = 1 mM. For PL spectra, λ_{ex} = 405 nm.

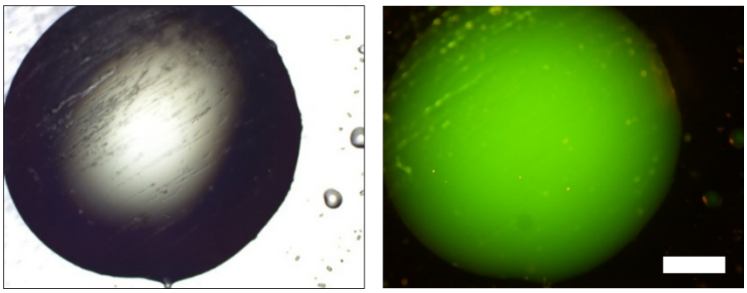

Figure S2. Optical and FM image of COPV doped ER. Scale bar: 150 μm.

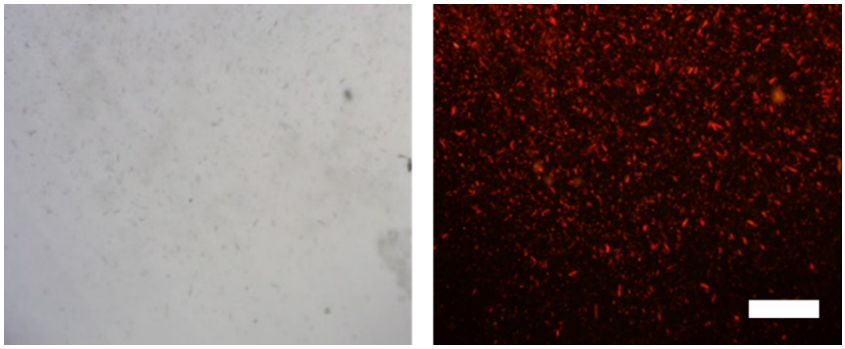

Figure S3. Optical and FM image of COPV doped PDMS. Scale bar: 150 µm.

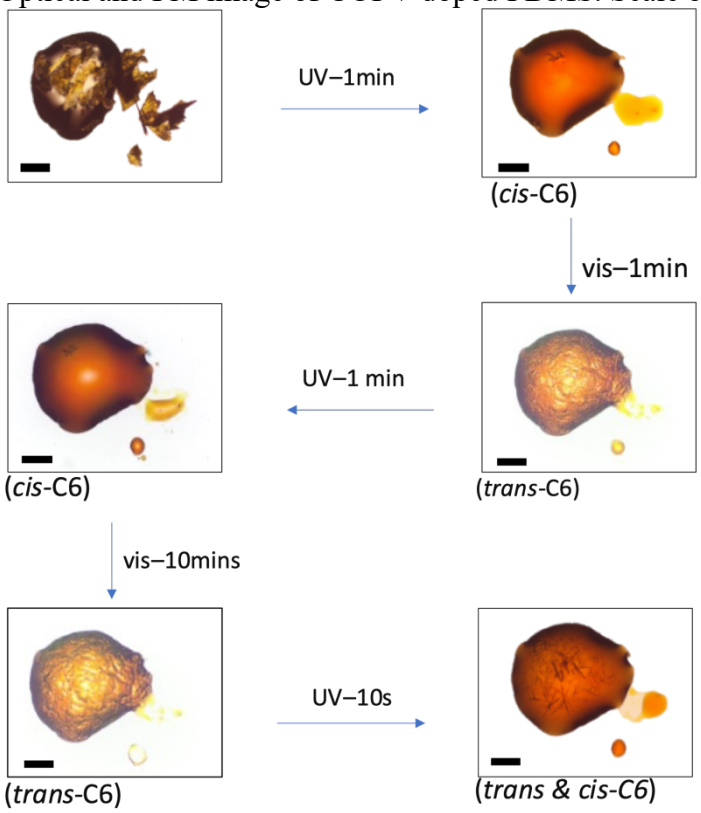

Figure S4. a) Optical microscope images of C6 and ER droplet during several cycles of UV and vis irradiation (λ_{UV} = 350–390 nm, λ_{vis} = 450–490 nm). Scale bars: 200 µm.

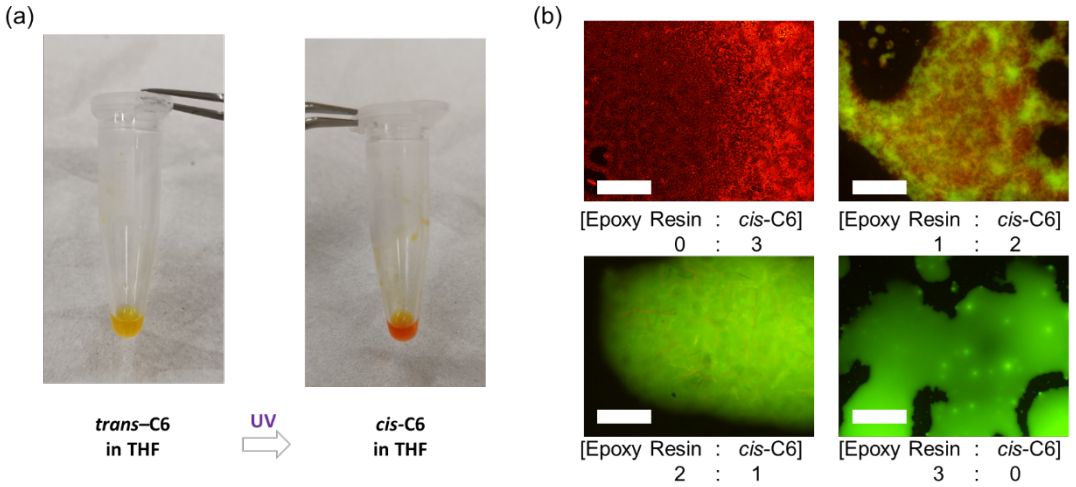

Figure S5. a) Photographs of C6 solution in THF before and after irradiation with UV-LED (λ_{ex} = 375 nm). b) FM image of mixture droplet from ER/*cis*-C6 with various ratios. Scale bars: 150 µm.

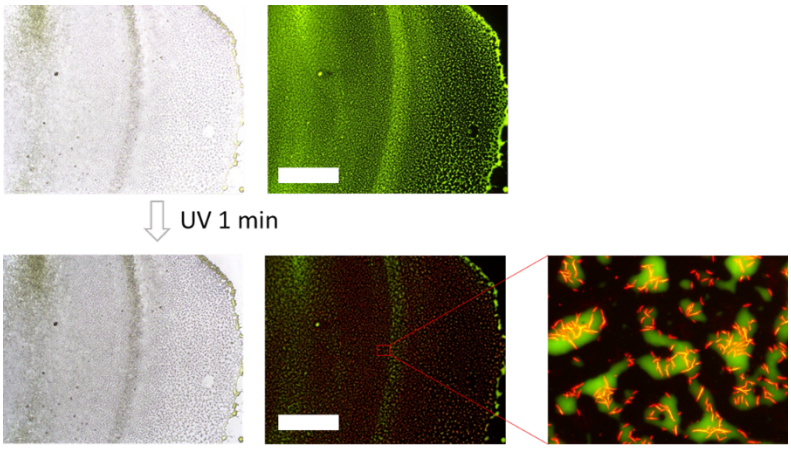

Figure S6. Optical and FM image of liquid film from COPV doped ER before and after irradiation with UV light (λ_{ex} = 350–390 nm. Scale bars: 100 μm.

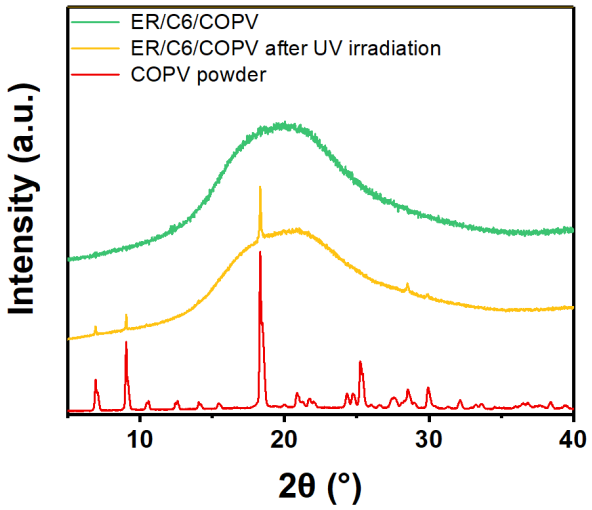

Figure S7. XRD patterns of COPV powder (red) and ER/C6/COPV before (green) and after (yellow) UV irradiation.

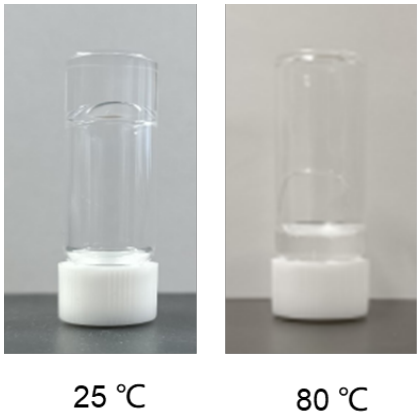

Figure S8. Photographs of ER after standing upside down for 5 s at different temperature.

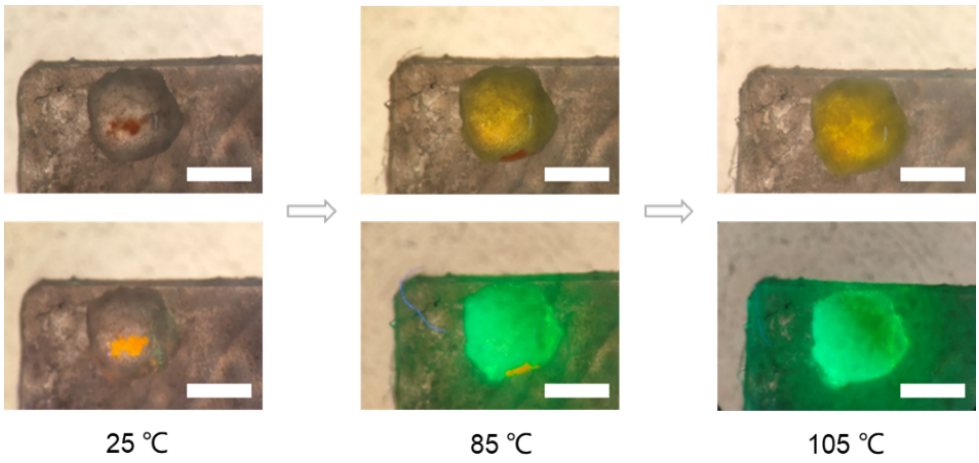

Figure S9. Photographs of ER droplet with COPV powder during heating process. Scale bars: 2 mm.

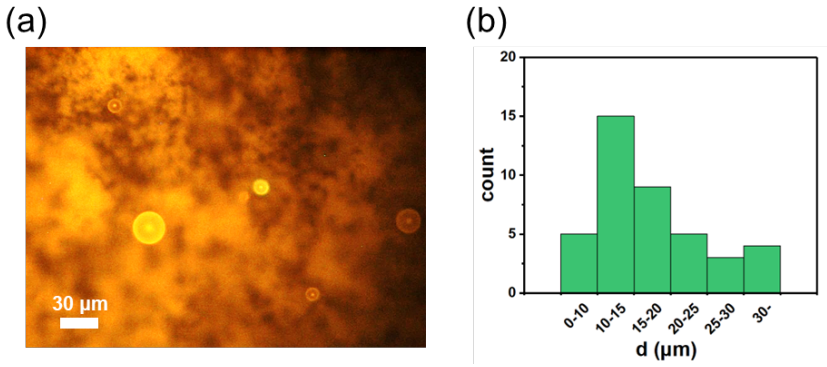

Figure S10. a) Optical microscope image of $\mathbf{MD_{ER\text{-}C6}}$. b) Histograms of *d* for $\mathbf{MD_{ER\text{-}C6}}$.

The microspheres with polystyrene (PS) as a matrix and COPVs as fluorescent dopants ($\mathbf{MS_{PS\text{-}COPV}}$) are fabricated by a common mini-emulsion method reported previously.[S1] For [PS] = 1 mg/mL, it can be seen from SEM image that $\mathbf{MS_{PS\text{-}COPV}}$ has a smooth surface morphology with a diameter (*d*) in a range of 1–5 μm (Figure S10a). Upon photoirradiation at λ_{ex} = 450–490 nm (Figure S10b), $\mathbf{MS_{PS\text{-}COPV}}$ shows green fluorescence, indicating well dispersed COPV with G-phase in the microsphere. The spectrum from G-phase $\mathbf{MS_{PS\text{-}COPV}}$ upon excitation with a focused laser beam (λ_{ex} = 455 nm) at the rim features periodic peaks that are superposed on a broad green PL band, which can be attributed to WGM mode resonance induced by the light confinement in the microspheres via total internal reflection at the polymer/air interface (Figure S10c). As *d* increases, FSR decreases because of the longer optical path, which is in line with the equation (1) for WGM resonator. A plot of FSR as a function of d^{-1} (Figure S10d) from a series of single $\mathbf{MS_{PS\text{-}COPV}}$ with *d* of 2–15 μm shows a linear relationship.

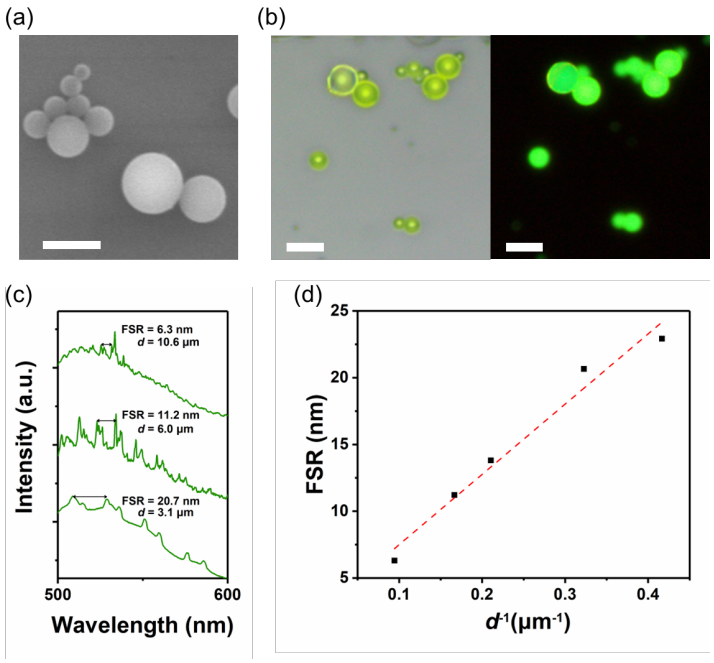

Figure S11. a) SEM image of $\mathbf{MS_{PS\text{-}COPV}}$. Scale bar: 5 μm. Optical and FM images (λ_{ex} = 460–495 nm) of $\mathbf{MS_{PS\text{-}COPV}}$. Scale bars: 5 μm. c) μ-PL spectra of single $\mathbf{MS_{PS\text{-}COPV}}$ with various diameters. d) Plot of the FSR versus d^{-1}. The red dashed line represents the fitting result.

The emission of multi-color AIE dyes is readily manipulated over a wide range by doping AIE dyes in host polymers and controlling the extent of aggregation.[S2] Due to the relatively low solubility of COPV in chloroform, a variety of [PS] (0.1–1 mg/mL) in precursor is used to tune the ratio of PS to COPVs. $\mathbf{MS_{PS\text{-}COPV}}$ with [PS] ranging from 1 to 0.1 mg mL^{-1} in precursor is successfully fabricated (insets of Figure S11). Upon decreasing [PS], the FM images of $\mathbf{MS_{PS\text{-}COPV}}$ display emission color change from bright green (1.0 and 0.8 mg mL^{-1} for PS) to yellowish green (0.6 and 0.4 mg mL^{-1} for PS) and then to yellow (0.2 mg mL^{-1} for PS) under irradiation at 450–490 nm. The variety of emission color can be attributed to the changing molecular configuration from G-phase to Y-phase of COPVs in PS matrix. When excited with a focused laser beam (λ = 455 nm), PL spectra exhibit a broad PL band overlapped with a set of sharp and periodic peaks. Noticeably, the main PL band shows an obvious shift from green (510 nm) to yellow (559 nm) region following the increased COPVs content in $\mathbf{MS_{PS\text{-}COPV}}$. But for [PS] = 0.1 mg mL^{-1}, the assembly of PS and COPVs tend to form unregular blocks due to the high content of crystalline COPVs, which displays bright red emission. PL spectrum hardly features periodic resonance peak due to irregular surface morphology.

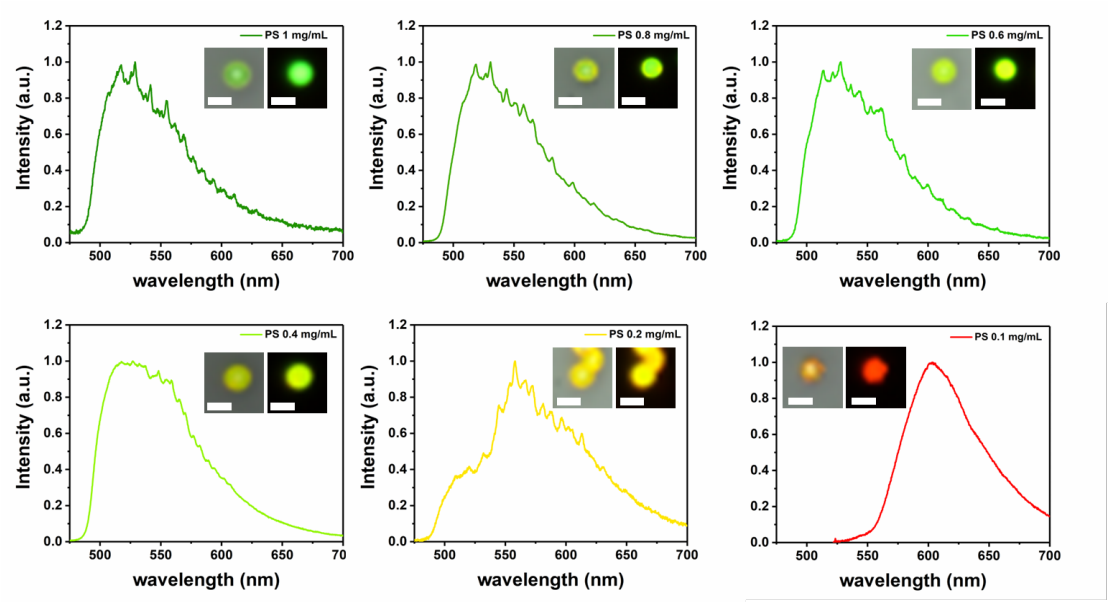

Figure S12. μ-PL spectra of single $\mathbf{MS_{PS\text{-}COPV}}$ with different PS content. Inserts are corresponding optical and FM images of $\mathbf{MS_{PS\text{-}COPV}}$. Scale bars: 5 μm.

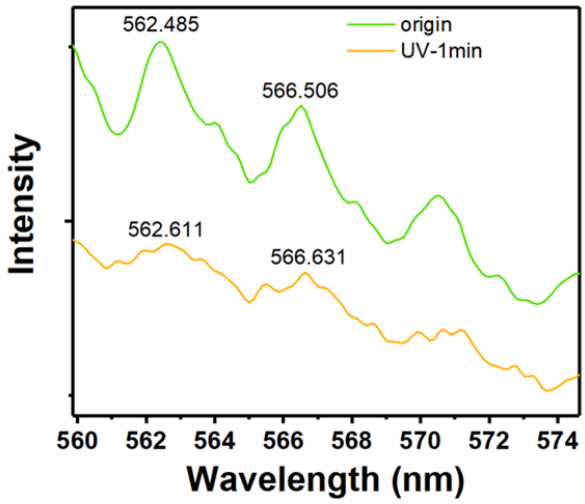

Figure S13. Magnified PL spectra of a single $\mathbf{MD_{ER\text{-}C6}}$.

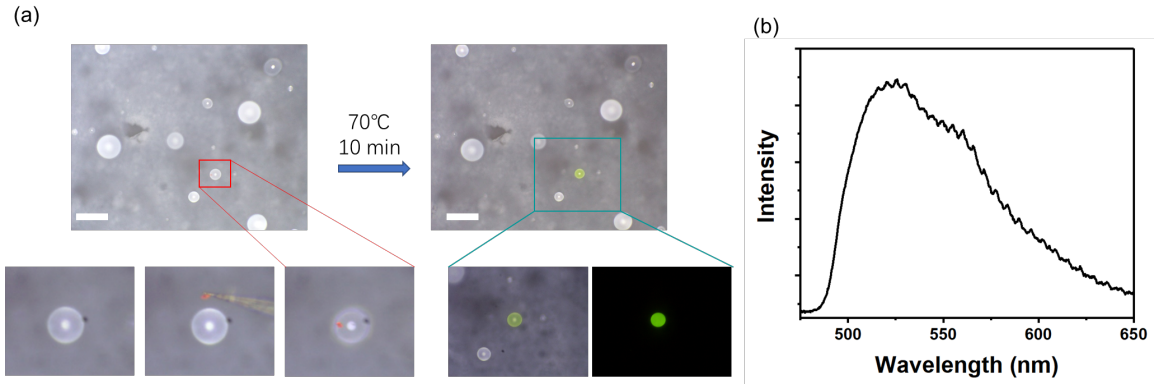

Figure S14. a) Optical and FM images of $\mathbf{MD_{ER}}$ with COPV microcrystal. Scale bar: 10 μm. b) μ-PL spectrum of $\mathbf{MD_{ER}}$ with dissolved COPV.

References

[S1] A. Qiagedeer, H. Yamagishi, S. Hayashi, Y. Yamamoto, *ACS Omega* **2021**, *6*, 21066.
[S2] C. Löwe, C. Weder, *Adv. Mater.* **2002**, *14*, 1625.